

Available online at www.sciencedirect.com

International Journal of Solids and Structures 44 (2007) 18–33

INTERNATIONAL JOURNAL OF
**SOLIDS and
STRUCTURES**www.elsevier.com/locate/ijsolstr

Interfacial stiffness dependence of the effective magnetostriction of particulate magnetostrictive composites

Yongping Wan ^{a,*}, Jinhao Qiu ^b, Zheng Zhong ^a^a *School of Aerospace Engineering and Applied Mechanics, Tongji University, No. 1239 Siping Road, 200092 Shanghai, People's Republic of China*^b *Institute of Fluid Science, Tohoku University, Katahira 2-1-1, Aoba-ku, Sendai 980-8577, Japan*Received 27 December 2005; received in revised form 31 March 2006
Available online 22 April 2006

Abstract

Terfenol-D composites attract much attention recently due to their large magnetostriction, small eddy energy loss and large operation frequency bandwidth. Binder layer in the composite usually mechanically weakens the composite and reduces the effective properties. A typical kind of magnetostrictive composite is composed of Rare Earth metallic compound powder, matrix material and resin binder. The binder, which is usually flexible and forms mechanically weak interface in the composite, inevitably influences the overall magnetostriction of composites. In this paper, a theoretical model was developed to treat a simple deformation case of this kind of mechanically weak interface, in which the flexible layer has low stiffness to withstand deformation but no de-bonding or cracking. An infinite magnetostrictive plane with a circular inclusion was considered, where the matrix and inclusion are all general magnetostrictive materials which can be modeled by the standard square constitutive relation of magnetostriction. The binder layer of a certain thickness was modeled as a set of springs with no thickness but with an equivalent stiffness. The mathematical formulation was brought into the complex variable framework. The magnetoelastic field was solved and the effective magnetostriction was explicitly obtained. Comparisons with experimental results were also presented. In terms of this analysis, the interfacial stiffness has significant influences on the overall magnetostriction of composite. Increasing the interfacial stiffness can lead to large magnetostriction of composites. The measure for improving the interfacial stiffness includes increasing the binder modulus and reducing its thickness.

© 2006 Elsevier Ltd. All rights reserved.

Keywords: Magnetostrictive composite; Binder; Flexible interfacial layer; Effective magnetostriction

1. Introduction

Magnetostrictive materials are important functional materials in modern smart devices. The classical magnetostrictive materials are usually the soft ferromagnetic metals such as the pure iron, nickel and so on, which

* Corresponding author. Tel.: +86 21 65982591.
E-mail address: wany@mail.tongji.edu.cn (Y. Wan).

have a small magnetostriction and, currently, are seldom employed in the modern magnetostrictively functional devices. The Rare Earth (RE) magnetostrictive alloy, the so-called Giant Magnetostrictive Materials, have attracted much attention in the past decades due to their very large magnetostriction, high energy density and quick response to external magnetic field (Clark, 1980). The RE metallic alloy, however, has very large eddy-current energy loss and is generally limited to several kilohertz frequency (Kendall and Piercy, 1993). Some adequately manipulated magnetostrictive composites can greatly reduce the eddy-current loss and improve mechanical properties while keeping relatively large magnetostriction. The magnetostrictive composite with resin matrix can be operated till several hundred kilohertz, which greatly extends frequency limit of magnetostrictive materials (Hudson et al., 1998).

There are usually several kinds of magnetostrictive composites, such as the 1–3 (Ren et al., 2005), 2–2 (Dong et al., 2005), and 0–3 type (Duenas and Carman, 2001). The 0–3 type composite can be obtained by mixing RE metallic alloy powder with some kind of matrix powder. If a magnetic field is used for orientation, magnetic particles inside the composite will be aligned like a fiber, forming the so-called pseudo-1–3 composite (Ren et al., 2005). The RE magnetostrictive layer and the piezoelectric layer are sometimes stacked and bonded to form the sandwiched laminate or multilayer actuators, which are of the 2–2 type (Dong et al., 2005).

Magnetostrictive composites with RE metallic particles have been investigated theoretically and experimentally. Herbst et al. (1997) studied the effective magnetostriction of composites by choosing $smFe_2$ as the magnetostrictive phase and adopting aluminum (Al) and iron (Fe) powder as matrix, respectively. A theoretical model was also proposed for predicting the effective magnetostriction of the composite with non-magnetostrictive matrix. Based on the Green's function, Nan (1998) developed a model for the effective magnetostriction, which actually treat the magnetostrictive behavior linearly. Chen et al. (1999) experimentally studied the magnetostrictive behavior of composites with different kinds of matrices, and gave a simple model to account for their experimental results based on the assumption of uniform stress and uniform strain. Guo et al. (2001) have conducted the experiment of Terfenol-D composite with epoxy resin as matrix. It was found that some previous models can not predict accurately the results. A model based on the strain energy consideration was then developed. As the RE magnetostrictive materials usually exhibit obvious nonlinear behavior under external magnetic field (Wan et al., 2003a; Zheng and Liu, 2005), Wan et al. (2004) included this nonlinear effect and developed a model for the effective magnetostriction for general magnetostrictive composites, where both matrix and inclusion are all magnetostrictive and modeled by the nonlinear constitutive relations.

To prepare magnetostrictive composites, the RE metallic alloy powder and the matrix are usually mixed together with some resin. The resin, which serves as the binder, greatly enhances the resistivity and reduces the eddy-current loss by isolating the metallic particles and avoiding the percolation path of metallic particles through the composite. The coating resin covering the RE alloy particles, which is very thin compared to the particle size, usually has a low modulus and actually forms a flexible interfacial layer between the matrix and metallic particles. Upon stresses, the flexible thin layer, which is usually mechanically weak compared to the matrix and inclusion, undergoes deformation and even sometimes comes to failure such as sliding, de-bonding, cracking etc. The deformation and failure inevitably bring influences on the properties of magnetostrictive composites (Kim et al., 1998). Therefore, similar to the ordinary composite, interfacial problems are also key to the overall properties of magnetostrictive composites and should be rigorously examined.

The above-mentioned theoretical models, however, did not consider the effect of flexible interface. The deformation and failure of flexible interface are generally very complicated in the composite. For a typical kind of composite with Terfenol-D as magnetostrictive phase and resin as the binder, in this paper, a theoretical model was developed to treat a simple deformation case of this kind of mechanically weak interface, in which the flexible layer has low stiffness to withstand deformation but no de-bonding or cracking occurs. This model, as compared to the perfect interface model (Wan et al., 2004) where the surface traction and displacements are continuous across the interface, takes force-dependent displacements on the interface and, to some extent, physically characterizes the flexible but non-breaking resin binder. A finite stiffness can be used to representing a certain kind of interfacial layer of resin. The perfect interface model can be mathematically recovered if the interfacial stiffness tends to be infinite.

An infinite magnetostrictive plane with an embedded circular inclusion was considered, where both the matrix and inclusion are magnetostrictive and modeled by the standard square constitutive relation of magnetostriction. The mathematical formulation was brought into the complex variable framework. The magnetic

and elastic fields were solved and the effective magnetostriction was explicitly obtained. Comparisons with experimental results were also made. The binder influences on the effective magnetostriction were analyzed, including the interfacial stiffness, material modulus and the thickness of the binder layer. In Section 2, the theoretical model is established and the mathematical formulation is presented in terms of the complex variable method. In Section 3, solution to this problem is obtained. The fourth section gives theoretical analysis and experimental verification. The final section is the conclusion of this paper.

2. Formulation

To study the influence of the mechanically-weak binder layer on the effective magnetostriction of the particulate composite, a planar model of magnetostrictive matrix with a circular inclusion is considered. As shown in Fig. 1, a circular magnetostrictive inclusion ($m_{\parallel}^I, G^I, \mu^I$) of radius, a , is embedded in an infinite magnetostrictive plane ($m_{\parallel}^M, G^M, \mu^M$) with a thin interfacial layer (E^b, ν^b) of thickness, Δ . This layer physically represents the resin binder in the composite, whose thickness is generally very small compared to the particle size, i.e. $\Delta \ll a$. At infinity, the mechanical load, σ^∞ , and the magnetic induction, B^∞ , are applied. The inclusion has the magnetostrictive coefficient of m_{\parallel}^I along the direction of external magnetic field, the shear modulus G^I , and permeability of μ^I , while the corresponding quantities of the matrix are denoted by m_{\parallel}^M, G^M and μ^M , respectively. E^b and ν^b are the Young's modulus and Poisson's ratio of the binder layer.

2.1. The magnetic induction

Magnetic materials exhibit magnetostriction under magnetic field. The elastic field in the magnetic material is influenced by the magnetic field through magnetostriction. The counter effect, however, is a high-order effect and can generally be believed to be relatively weak (Pao and Yeh, 1973; Wan et al., 2003b). The magnetic induction can be obtained without taking the magnetoelastic coupling into consideration. It can be reasonably assumed that a nonmagnetic inhomogeneous layer also exerts negligibly small disturbance to the distribution of magnetic field if the layer becomes very thin compared to the matrix and inclusion. Therefore, the magnetic field can be obtained from the rigid body configuration, where the thin nonmagnetic inhomogeneous layer is not considered. For a circular inclusion embedded in an infinite plane, the distribution of magnetic induction was already obtained by means of the complex variable method as follows (Wan et al., 2004):

$$w_M(z) = -\overline{B^\infty}z + \Pi \frac{a^2}{z}, \quad (1a)$$

$$w_I(z) = -\Gamma z, \quad (1b)$$

where $z = x_1 + ix_2$, $i = \sqrt{-1}$, x_1 and x_2 are the rectangular coordinates, an over bar represents conjugate of complex variables.

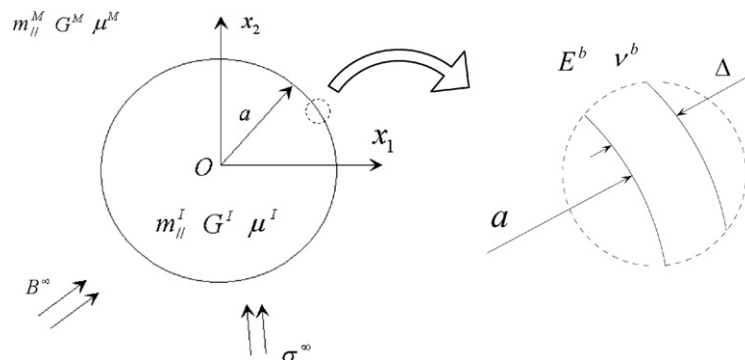


Fig. 1. A circular inclusion embedded in an infinite magnetostrictive plane with a thin layer (thickness of Δ).

$$\Gamma = \frac{2\mu^I \overline{B^\infty}}{\mu^I + \mu^M}, \tag{2a}$$

$$\Pi = \frac{(\mu^I - \mu^M)B^\infty}{\mu^I + \mu^M}, \tag{2b}$$

μ^I, μ^M are the permeability of inclusion and matrix, respectively. B^∞ is the magnetic induction at infinity. $w_I(z)$ and $w_M(z)$ are the complex potentials of magnetic induction in the inclusion and matrix, respectively. The magnetic induction can be obtained in terms of the complex potentials as follows:

$$B = -\overline{w'(z)}, \tag{3a}$$

where a prime denotes derivative with respect to the complex variable, z .

$$B = B_1 + iB_2 \tag{3b}$$

in which B_1 and B_2 are components of the magnetic induction along the coordinate axes.

2.2. The mechanical interfacial conditions

Though the magnetic induction is assumed to be insensitive to the presence of a nonmagnetic thin layer, the elastic field, however, may be very sensitive to this interfacial layer due to mechanical weakness. Therefore, the elastic field should be solved in terms of the boundary conditions including the mechanically weak thin layer. The mechanical conditions can be established by examining the deformation of the binder layer. As shown in Figs. 2 and 3, the small deformation of a unit cell with the area dA of the binder layer can be divided into two parts, i.e. the normal elongation (Fig. 2) and the shear deformation (Fig. 3). In this paper, the binder layer was theoretically treated by means of the equivalent models (Figs. 2b and 3b), in which the binder layer of thickness Δ is replaced by a set of springs and additional matrix layer of thickness Δ . The set of springs, which is

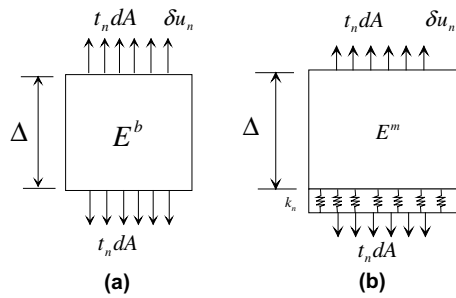


Fig. 2. The normal elongation: (a) the physical model and (b) the equivalent model.

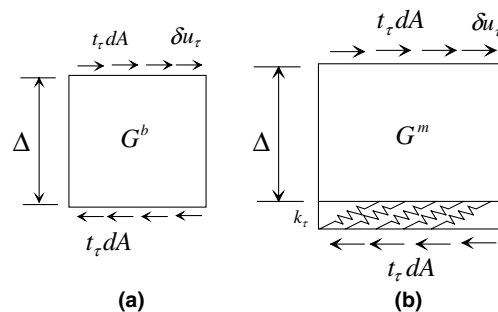


Fig. 3. The shear deformation: (a) the physical model and (b) the equivalent model.

considered to take up no space, have the normal stiffness k_n and the tangential stiffness k_τ . To determine the stiffness of the interface, k_n and k_τ , the traction and displacement responses of the equivalent model are equated to those of the physical model.

The relative displacement in the normal direction of the physical model, δu_n , as shown in Fig. 2a, is as follows:

$$\delta u_n = \frac{t_n dA}{dA} \frac{\Delta}{E^b}, \quad (4a)$$

where E^b is the Young's modulus of the binder, t_n is the traction in the normal direction. The relative displacement in the normal direction of the equivalent model, δu_n , as shown in Fig. 2b, is given by

$$\delta u_n = \frac{t_n dA}{dA} \frac{1}{k_n} + \frac{t_n dA}{dA} \frac{\Delta}{E^M}, \quad (4b)$$

where E^M is the Young's modulus of the matrix. The normal stiffness can be solved by means of equating Eqs. (4a) to (4b).

$$k_n = \frac{E^b}{\Delta} \frac{1}{1 - E^b/E^M}. \quad (5)$$

Similarly, the relative displacement in the tangential direction δu_τ , in Fig. 3a and b, are given as follows:

$$\delta u_\tau = \frac{t_\tau dA}{dA} \frac{\Delta}{G^b}, \quad (6a)$$

$$\delta u_\tau = \frac{t_\tau dA}{dA} \frac{1}{k_\tau} + \frac{t_\tau dA}{dA} \frac{\Delta}{G^M}, \quad (6b)$$

where G^b and G^M are the shear modulus of the binder and the matrix, respectively. t_τ is the traction in the tangential direction. The tangential stiffness can be obtained by considering the equivalence of the displacements in Eqs. (6a) and (6b).

$$k_\tau = \frac{G^b}{\Delta} \frac{1}{1 - G^b/G^M}. \quad (7)$$

The mechanical conditions of this problem are actually the deformation equations of the springs, which are considered taking up no space between the inclusion and the matrix. These deformation equations include the surface tractions which are relative-displacement dependent, both in the normal and tangential direction, and the interface conditions of the surface tractions.

$$t_n^I - k_n(u_n^I - u_n^M) = 0, \quad (8a)$$

$$t_\tau^I - k_\tau(u_\tau^I - u_\tau^M) = 0, \quad (8b)$$

$$\mathbf{t}^I + \mathbf{t}^M = \mathbf{0}, \quad (8c)$$

where the symbols I and M are used to denoting the quantities of inclusion and matrix, respectively. \mathbf{t} is the surface traction vector. The letter in bold type refers to the vector or tensor in this paper. The interface conditions of the surface tractions in Eq. (8c) can also be presented with the stresses of the inclusion and the matrix.

$$\mathbf{n}^I \cdot \boldsymbol{\sigma}^I + \mathbf{n}^M \cdot \boldsymbol{\sigma}^M = 0, \quad (9)$$

where $\boldsymbol{\sigma}^I$ and $\boldsymbol{\sigma}^M$ are the stress tensor in the inclusion and matrix, respectively. \mathbf{n}^I and \mathbf{n}^M the unit outward normal to the interface for the inclusion and that for the matrix, respectively. Note that these two units outward normal to the interface are exactly the same in magnitude but opposite in direction, i.e.

$$\mathbf{n}^M = -\mathbf{n}^I. \quad (10)$$

Substituting Eq. (10) into Eq. (9) and using \mathbf{n} to representing for \mathbf{n}^I , the surface traction conditions in Eq. (8c) can also be written into the following form:

$$\mathbf{n} \cdot (\boldsymbol{\sigma}^I - \boldsymbol{\sigma}^M) = 0, \quad (11)$$

where \mathbf{n} represents the unit outward normal to the interface for the inclusion.

It can be seen from Eqs. (5) and (7) that the interface stiffness is usually finite for a general case where the binder is of a certain thickness and compliant compared with the matrix. There are two limit cases where the interface stiffness tends to be infinite. One is when the thickness reduces to zero and the binder vanishes, another is when the binder material is identical to the matrix. In both cases the tractions and the displacements are continuous across the interface, and this model recovers the perfect interface model (Wan et al., 2004).

2.3. Complex variable framework

The 2-dimensional standard square constitutive relation of magnetostriction is (Wan et al., 2004)

$$\varepsilon_{\alpha\beta} = \frac{1+\nu}{E}(\sigma_{\alpha\beta} - \nu\sigma_{\gamma\gamma}\delta_{\alpha\beta}) + (m_{\parallel} - m_{\perp})B_{\alpha}B_{\beta} + (1+\nu)m_{\perp}B_{\gamma}B_{\gamma}\delta_{\alpha\beta}, \quad (12)$$

where α, β and γ run from 1 to 2, $\sigma_{\alpha\beta}$ is the stress tensor, $\varepsilon_{\alpha\beta}$ the strain tensor, B_{α} the magnetic induction, $\delta_{\alpha\beta}$ the Kronecker delta. m_{\parallel} and m_{\perp} are, respectively, the magnetostrictive coefficients along the direction of applied magnetic field and its perpendicular direction. E and ν are the Young's modulus and the Poisson's ratio, respectively. The equilibrium equation and the geometric compatibility equation are as follows:

$$\sigma_{\alpha\beta,\beta} = 0, \quad (13a)$$

$$\varepsilon_{\alpha\beta} = \frac{1}{2}(u_{\alpha,\beta} + u_{\beta,\alpha}), \quad (13b)$$

in which u_{α} ($\alpha = 1, 2$) are the displacements. A prime denotes the derivative with respect to the coordinates x_{α} . The conventional summation rule is adopted. The constitutive equation in (12), together with the field equation in (13a) and (13b), constitutes the problem of magnetostrictive elasticity. This problem can be solved within the framework of complex potentials (see Appendix A).

The surface tractions and displacements in the normal and tangential direction can be obtained respectively through the stress and displacement components by means of the following equations:

$$t_n^I = n_1^2\sigma_{11}^I + n_2^2\sigma_{22}^I + 2n_1n_2\sigma_{12}^I, \quad (14a)$$

$$t_{\tau}^I = n_1n_2(\sigma_{11}^I - \sigma_{22}^I) + (n_2^2 - n_1^2)\sigma_{12}^I, \quad (14b)$$

$$u_n^I = u_1^In_1 + u_2^In_2, \quad (14c)$$

$$u_{\tau}^I = u_1^In_2 - u_2^In_1, \quad (14d)$$

$$u_n^M = u_1^Mn_1 + u_2^Mn_2, \quad (14e)$$

$$u_{\tau}^M = u_1^Mn_2 - u_2^Mn_1, \quad (14f)$$

where σ_{11} , σ_{22} and σ_{12} are the stress components, u_1 and u_2 are the displacement components. The superscripts I and M denote the quantities for the inclusion and matrix, respectively. n_1 and n_2 are the directional cosines of the unit outward normal to the interface for the inclusion, which can be expressed in terms of the complex variables,

$$n_1 = \frac{1}{ds} \left[\frac{1}{2i} (dz - d\bar{z}) \right], \quad (15a)$$

$$n_2 = -\frac{1}{ds} \left[\frac{1}{2} (dz + d\bar{z}) \right], \quad (15b)$$

where $\bar{z} = x_1 - ix_2$ is the conjugate of z . ds the differential of arc length. With reference to Eqs. (14) and (15) and the resultant forces of the surface tractions along the interface, the mechanical interfacial conditions in Eqs. (8a), (8b) and (11) can be re-written with complex variables as follows:

$$\left(\frac{dz}{d\bar{z}}\right)[(\sigma_{22} - \sigma_{11}) + 2\sigma_{12}i]_I + \overline{\left(\frac{dz}{d\bar{z}}\right)[(\sigma_{22} - \sigma_{11}) + 2\sigma_{12}i]_I} + 2(\sigma_{22} + \sigma_{11})_I + 2k_n i \left\{ \overline{\left(\frac{d\bar{z}}{dz}\right)^{\frac{1}{2}} [(u_1 + iu_2)_I - (u_1 + iu_2)_M]} - \left(\frac{d\bar{z}}{dz}\right)^{\frac{1}{2}} [(u_1 + iu_2)_I - (u_1 + iu_2)_M]} \right\} = 0, \quad (16a)$$

$$i \left\{ \left(\frac{dz}{d\bar{z}}\right)[(\sigma_{22} - \sigma_{11}) + 2\sigma_{12}i]_I - \overline{\left(\frac{dz}{d\bar{z}}\right)[(\sigma_{22} - \sigma_{11}) + 2\sigma_{12}i]_I} \right\} + 2k_\tau \left\{ \overline{\left(\frac{d\bar{z}}{dz}\right)^{\frac{1}{2}} [(u_1 + iu_2)_I - (u_1 + iu_2)_M]} + \left(\frac{d\bar{z}}{dz}\right)^{\frac{1}{2}} [(u_1 + iu_2)_I - (u_1 + iu_2)_M]} \right\} = 0, \quad (16b)$$

$$\Omega_I(z) + z\overline{\Omega'_I(z)} + \overline{\Psi_I(z)} - \frac{S^I}{2} w_1(z)\overline{w'_1(z)} = \Omega_M(z) + z\overline{\Omega'_M(z)} + \overline{\Psi_M(z)} - \frac{S^M}{2} w_M(z)\overline{w'_M(z)}, \quad (16c)$$

where $\Omega_I(z)$, $\Psi_I(z)$, $\Omega_M(z)$ and $\Psi_M(z)$ are the complex potentials in the circular inclusion and outside matrix, respectively. The displacements and stresses expressed with complex potentials are listed in Appendix A. It should be noted that both sides of Eq. (16c) are complex, which actually represents two identities. For the sake of convenience, the interfacial conditions are transformed into the ζ plane with the mapping function, $z = a\zeta$, where the complex potentials assume the following forms:

$$\Omega_I(z) = \Omega_I^0(\zeta), \quad (17a)$$

$$\Psi_I(z) = \Psi_I^0(\zeta), \quad (17b)$$

$$\Omega_M(z) = p_1 z + \Omega_M^0(\zeta), \quad (18a)$$

$$\Psi_M(z) = p_2 z + \Psi_M^0(\zeta), \quad (18b)$$

where p_1, p_2 are determined by the remote magnetic and mechanical loads.

$$p_1 = \frac{S^M}{4} \Pi \bar{\Pi}, \quad (19a)$$

$$p_2 = \frac{\sigma_{22}^\infty - \sigma_{11}^\infty + 2i\sigma_{12}^\infty}{4}. \quad (19b)$$

The interface between the matrix and inclusion in the physical plane, i.e. $z\bar{z} = a^2$, is mapped to be the unit circle, $\sigma = e^{i\theta}$, in the ζ plane, where there is $\bar{\sigma} = 1/\sigma$. The interfacial conditions in Eqs. (16a)–(16c) become as follows:

$$\begin{aligned} & \frac{2}{a} \left[\sigma \Omega_I^{0'}(\sigma) + \frac{1}{\sigma} \overline{\Omega_I^{0'}(\sigma)} \right] + \frac{2}{a} \left[\sigma^2 \Psi_I^{0'}(\sigma) + \frac{1}{\sigma^2} \overline{\Psi_I^{0'}(\sigma)} \right] - \frac{4}{a} \left[\Omega_I^{0'}(\sigma) + \overline{\Omega_I^{0'}(\sigma)} \right] \\ & - k_n \left\{ \frac{3 - 4\nu^I}{G^I} \left[\frac{1}{\sigma} \Omega_I^0(\sigma) + \sigma \overline{\Omega_I^0(\sigma)} \right] - \frac{3 - 4\nu^M}{G^M} \left[\frac{1}{\sigma} \Omega_M^0(\sigma) + \sigma \overline{\Omega_M^0(\sigma)} \right] \right. \\ & - \frac{1}{G^I} \left[\Omega_I^{0'}(\sigma) + \overline{\Omega_I^{0'}(\sigma)} \right] + \frac{1}{G^M} \left[\Omega_M^{0'}(\sigma) + \overline{\Omega_M^{0'}(\sigma)} \right] - \frac{1}{G^I} \left[\sigma \Psi_I^0(\sigma) + \frac{1}{\sigma} \overline{\Psi_I^0(\sigma)} \right] \\ & \left. + \frac{1}{G^M} \left[\sigma \Psi_M^0(\sigma) + \frac{1}{\sigma} \overline{\Psi_M^0(\sigma)} \right] \right\} + L_{12} \sigma^2 + \overline{L_{12}} \frac{1}{\sigma^2} + L_{10} = 0, \quad (20a) \end{aligned}$$

$$\begin{aligned} & \frac{2}{a} \left[\frac{1}{\sigma} \overline{\Omega_1^{0''}(\sigma)} - \sigma \overline{\Omega_1^{0''}(\sigma)} \right] + \frac{2}{a} \left[\frac{1}{\sigma^2} \overline{\Psi_1^{0''}(\sigma)} - \sigma^2 \overline{\Psi_1^{0''}(\sigma)} \right] \\ & - k_\tau \left\{ \frac{3-4\nu^I}{G^I} \left[\frac{1}{\sigma} \overline{\Omega_1^0(\sigma)} - \sigma \overline{\Omega_1^0(\sigma)} \right] - \frac{3-4\nu^M}{G^M} \left[\frac{1}{\sigma} \overline{\Omega_M^0(\sigma)} - \sigma \overline{\Omega_M^0(\sigma)} \right] \right. \\ & - \frac{1}{G^I} \left[\overline{\Omega_1^{0'}(\sigma)} - \Omega_1^{0'}(\sigma) \right] + \frac{1}{G^M} \left[\overline{\Omega_M^{0'}(\sigma)} - \Omega_M^{0'}(\sigma) \right] \\ & \left. - \frac{1}{G^I} \left[\frac{1}{\sigma} \overline{\Psi_1^0(\sigma)} - \sigma \overline{\Psi_1^0(\sigma)} \right] + \frac{1}{G^M} \left[\frac{1}{\sigma} \overline{\Psi_M^0(\sigma)} - \sigma \overline{\Psi_M^0(\sigma)} \right] \right\} + \overline{L_{22}} \frac{1}{\sigma^2} - L_{22} \sigma^2 = 0, \end{aligned} \quad (20b)$$

$$\left[\overline{\Omega_1^0(\sigma)} - \Omega_M^0(\sigma) \right] + \sigma \left[\overline{\Omega_1^{0'}(\sigma)} - \overline{\Omega_M^{0'}(\sigma)} \right] + \left[\overline{\Psi_1^0(\sigma)} - \overline{\Psi_M^0(\sigma)} \right] - R_1 \sigma - R_2 \frac{1}{\sigma} + R_3 \sigma^3 = 0, \quad (20c)$$

where there are

$$L_{10} = -k_n a \left[\frac{S^I}{G^I} \Gamma \overline{\Gamma} - 2(1-\nu^M) \frac{S^M}{G^M} B^\infty \overline{B^\infty} + \frac{S^M}{G^M} \Pi \overline{\Pi} + 2(m_{\parallel}^M - m_{\perp}^M) B^\infty \overline{\Pi} \right] + 2S^I \Gamma \overline{\Gamma}, \quad (21a)$$

$$L_{12} = -k_n a \left\{ \frac{(m_{\parallel}^M - m_{\perp}^M)}{2} \left[\frac{1}{3} (\overline{\Pi})^2 - (\overline{B^\infty})^2 \right] + \frac{(m_{\parallel}^I - m_{\perp}^I)}{2} (\Gamma)^2 + \frac{\overline{p_2}}{G^M} \right\}, \quad (21b)$$

$$L_{22} = -k_\tau a \left\{ \frac{S^M}{G^M} \overline{B^\infty \Pi} - \frac{(m_{\parallel}^M - m_{\perp}^M)}{2} \left[\frac{1}{3} (\overline{\Pi})^2 + (\overline{B^\infty})^2 \right] + \frac{(m_{\parallel}^I - m_{\perp}^I)}{2} (\Gamma)^2 + \frac{\overline{p_2}}{G^M} \right\}, \quad (21c)$$

$$R_1 = a \left(\frac{S^I}{2} \Gamma \overline{\Gamma} + \frac{S^M}{2} \Pi \overline{\Pi} \right), \quad (21d)$$

$$R_2 = a \left(\frac{S^M}{2} B^\infty \Pi + p_2 \right), \quad (21e)$$

$$R_3 = a \frac{S^M}{2} \overline{B^\infty \Pi}, \quad (21f)$$

The dimension of L_{10} , L_{12} and L_{22} are the same as that of stresses, while R_k ($k = 1, 2, 3$) have the dimension of the stress multiplied by length. In the above equations, the symbol S is defined as:

$$S = \frac{1 - (1 + 2\nu)q}{4} \frac{E}{1 - \nu^2} m_{\parallel}, \quad (22)$$

where $q = -m_{\perp}/m_{\parallel}$ named the magnetic Poisson's ratio, The superscripts or subscripts M and I refer to the quantities of matrix and the inclusion, respectively. σ_{11}^∞ , σ_{12}^∞ and σ_{22}^∞ are the mechanical loads applied at infinity.

3. Solutions and the effective magnetostriction

To solve the simultaneous Eqs. in (20a)–(20c), the unknown functions, $\Omega_M^0(\zeta)$, $\Psi_M^0(\zeta)$, $\Omega_I^0(\zeta)$ and $\Psi_I^0(\zeta)$, are expanded into series, of which $\Omega_M^0(\zeta)$ and $\Psi_M^0(\zeta)$ are defined outside the unit circle and can be expanded into the negative power series of ζ , while $\Omega_I^0(\zeta)$ and $\Psi_I^0(\zeta)$ are defined inside the unit circle and can be expanded into the positive power series of ζ .

$$\Omega_M^0(\zeta) = a_0 + \sum_{j=1}^{\infty} \frac{a_j}{\zeta^j}, \quad (23a)$$

$$\Psi_M^0(\zeta) = b_0 + \sum_{j=1}^{\infty} \frac{b_j}{\zeta^j}, \quad (23b)$$

$$\Omega_1^0(\zeta) = c_0 + \sum_{j=1}^{\infty} c_j \zeta^j, \quad (23c)$$

$$\Psi_1^0(\zeta) = d_0 + \sum_{j=1}^{\infty} d_j \zeta^j. \quad (23d)$$

Insert the power series into Eqs. (20a)–(20c), the simultaneous equations of the coefficients can be obtained as follows, from which the coefficients can be solved.

$$-\frac{k_n}{G^M}(b_1 + \bar{b}_1) - \left[\frac{k_n}{G^I}(2 - 4v^I) + \frac{4}{a} \right] (c_1 + \bar{c}_1) + L_{10} = 0, \quad (24a)$$

$$\frac{k_\tau}{G^M}(b_1 - \bar{b}_1) - \frac{k_n}{G^I}(4 - 4v^I)(c_1 - \bar{c}_1) + L_{20} = 0, \quad (24b)$$

$$-\bar{b}_1 + c_1 + \bar{c}_1 - R_1 = 0, \quad (24c)$$

$$\frac{k_n}{G^M}(4 - 4v^M)\bar{a}_1 - \frac{k_n}{G^M}\bar{b}_3 + \frac{k_n}{G^I}4v^I c_3 + \left(\frac{2}{a} + \frac{k_n}{G^I} \right) d_1 + L_{12} = 0, \quad (25a)$$

$$\frac{k_\tau}{G^M}(2 - 4v^M)\bar{a}_1 + \frac{k_\tau}{G^M}\bar{b}_3 + \left[\frac{k_\tau}{G^I}(6 - 4v^M) + \frac{12}{a} \right] c_3 + \left(\frac{k_\tau}{G^I} + \frac{2}{a} \right) d_1 + L_{22} = 0, \quad (25b)$$

$$\bar{a}_1 - \bar{b}_3 + c_3 + R_3 = 0, \quad (25c)$$

$$-\bar{a}_1 + 3c_3 + d_1 - \bar{R}_2 = 0. \quad (25d)$$

The coefficients b_1 and c_1 can be solved from Eqs. (24a)–(24c) as follows:

$$b_1 = \frac{2 \frac{k_n}{G^M} R_1 + L_{10}}{\frac{k_n}{G^I}(2 - 4v^I) + \frac{4}{a} + 2 \frac{k_n}{G^M}} - R_1, \quad (26a)$$

$$c_1 = \frac{2 \frac{k_n}{G^M} R_1 + L_{10}}{\frac{k_n}{G^I}(4 - 8v^I) + \frac{8}{a} + 4 \frac{k_n}{G^M}}. \quad (26b)$$

It can be verified that both b_1 and c_1 are real numbers. Similarly, the coefficients a_1 , b_3 , c_3 and d_1 can be obtained from Eqs. (25a)–(25d).

$$\begin{aligned} a_1 = & \left\{ \left[\frac{k_\tau}{G^M} + \frac{6}{a} + \frac{k_\tau}{G^I}(3 - 4v^I) \right] \cdot \left[\frac{k_n}{G^M} \bar{R}_3 - \left(\frac{k_n}{G^I} + \frac{2}{a} \right) R_2 - \bar{L}_{12} \right] \right. \\ & \left. - \left[\frac{k_\tau}{G^M} \bar{R}_3 + \left(\frac{k_\tau}{G^I} + \frac{2}{a} \right) R_2 + \bar{L}_{22} \right] \cdot \left[\frac{k_n}{G^M} + \frac{k_n}{G^I}(3 - 4v^I) + \frac{6}{a} \right] \right\} \\ & \cdot \left\{ \left[\frac{k_\tau}{G^M} + \frac{6}{a} + \frac{k_\tau}{G^I}(3 - 4v^I) \right] \cdot \left[\frac{k_n}{G^M}(3 - 4v^M) + \frac{2}{a} + \frac{k_n}{G^I} \right] \right. \\ & \left. + \left[\frac{k_\tau}{G^M}(3 - 4v^M) + \frac{k_\tau}{G^I} + \frac{2}{a} \right] \cdot \left[\frac{k_n}{G^M} + \frac{k_n}{G^I}(3 - 4v^I) + \frac{6}{a} \right] \right\}^{-1}, \end{aligned} \quad (27a)$$

$$\begin{aligned} b_3 = & \left\{ \left[\frac{k_\tau}{G^M}(2 - 4v^M) - \frac{4}{a} - \frac{k_\tau}{G^I}(2 - 4v^I) \right] \cdot \left[-\frac{k_n}{G^M} \bar{R}_3 + \left(\frac{k_n}{G^I} + \frac{2}{a} \right) R_2 + \bar{L}_{12} \right] \right. \\ & \left. - \left[\frac{k_\tau}{G^M} \bar{R}_3 + \left(\frac{k_\tau}{G^I} + \frac{2}{a} \right) R_2 + \bar{L}_{22} \right] \cdot \left[\frac{k_n}{G^M}(4 - 4v^M) + \frac{k_n}{G^I}(4 - 4v^I) + \frac{8}{a} \right] \right\} \\ & \cdot \left\{ \left[\frac{k_\tau}{G^M} + \frac{6}{a} + \frac{k_\tau}{G^I}(3 - 4v^I) \right] \cdot \left[\frac{k_n}{G^M}(3 - 4v^M) + \frac{2}{a} + \frac{k_n}{G^I} \right] \right. \\ & \left. + \left[\frac{k_\tau}{G^M}(3 - 4v^M) + \frac{k_\tau}{G^I} + \frac{2}{a} \right] \cdot \left[\frac{k_n}{G^M} + \frac{k_n}{G^I}(3 - 4v^I) + \frac{6}{a} \right] \right\}^{-1} + \bar{R}_3, \end{aligned} \quad (27b)$$

$$\begin{aligned}
 c_3 = & - \left\{ \left[\frac{k_n}{G^M} (3 - 4v^M) + \frac{2}{a} + \frac{k_n}{G^I} \right] \cdot \left[\frac{k_\tau}{G^M} R_3 + \left(\frac{k_\tau}{G^I} + \frac{2}{a} \right) \overline{R}_2 + L_{22} \right] \right. \\
 & + \left. \left[\frac{k_\tau}{G^M} (3 - 4v^M) + \frac{2}{a} + \frac{k_\tau}{G^I} \right] \cdot \left[\frac{k_n}{G^M} R_3 - \left(\frac{k_n}{G^I} + \frac{2}{a} \right) \overline{R}_2 - L_{12} \right] \right\} \\
 & \cdot \left\{ \left[\frac{k_\tau}{G^M} + \frac{6}{a} + \frac{k_\tau}{G^I} (3 - 4v^I) \right] \cdot \left[\frac{k_n}{G^M} (3 - 4v^M) + \frac{2}{a} + \frac{k_n}{G^I} \right] \right. \\
 & + \left. \left[\frac{k_\tau}{G^M} (3 - 4v^M) + \frac{k_\tau}{G^I} + \frac{2}{a} \right] \cdot \left[\frac{k_n}{G^M} + \frac{k_n}{G^I} (3 - 4v^I) + \frac{6}{a} \right] \right\}^{-1}, \tag{27c}
 \end{aligned}$$

$$\begin{aligned}
 d_1 = & \left\{ \left[\frac{k_\tau}{G^M} (10 - 12v^M) + \frac{12}{a} + \frac{k_\tau}{G^I} (6 - 4v^I) \right] \cdot \left[\frac{k_n}{G^M} R_3 - \left(\frac{k_n}{G^I} + \frac{2}{a} \right) \overline{R}_2 - L_{12} \right] \right. \\
 & + \left. \left[\frac{k_\tau}{G^M} R_3 + \left(\frac{k_\tau}{G^I} + \frac{2}{a} \right) \overline{R}_2 + L_{22} \right] \cdot \left[\frac{k_n}{G^M} (8 - 12v^M) + \frac{k_n}{G^I} 4v^I \right] \right\} \\
 & \cdot \left\{ \left[\frac{k_\tau}{G^M} + \frac{6}{a} + \frac{k_\tau}{G^I} (3 - 4v^I) \right] \cdot \left[\frac{k_n}{G^M} (3 - 4v^M) + \frac{2}{a} + \frac{k_n}{G^I} \right] \right. \\
 & + \left. \left[\frac{k_\tau}{G^M} (3 - 4v^M) + \frac{k_\tau}{G^I} + \frac{2}{a} \right] \cdot \left[\frac{k_n}{G^M} + \frac{k_n}{G^I} (3 - 4v^I) + \frac{6}{a} \right] \right\}^{-1} + \overline{R}_2. \tag{27d}
 \end{aligned}$$

All other coefficients are zero. The detailed derivation is given in Appendix B. Therefore, there are only six non-zero coefficients remained, i.e. a_1, b_1, c_1, d_1, b_3 and c_3 . The complex potentials can be obtained in the physical plane (z plane) by means of the inverse transform, and listed as follows:

$$\Omega_M(z) = p_1 z + a_1 \frac{a}{z}, \tag{28a}$$

$$\Psi_M(z) = p_2 z + b_1 \frac{a}{z} + b_3 \frac{a^3}{z^3}, \tag{28b}$$

$$\Omega_I(z) = c_1 \frac{z}{a} + c_3 \frac{z^3}{a^3}, \tag{28c}$$

$$\Psi_I(z) = d_1 \frac{z}{a}. \tag{28d}$$

The elastic field of this problem can be obtained by inserting the complex potentials (28a)–(28d) into the equations in Appendix A. To obtain the magnetostriction of composite, without loss of any generality, a special case is discussed where the external magnetic field is directed along the x_2 axis, i.e. $B^\infty = iB_2^\infty$, and no mechanical loads are exerted at infinity. The displacement field is obtained as follows:

$$u_1^M = u_1^I = 0, \tag{29a}$$

$$\begin{aligned}
 u_2^M = & \left[\frac{2 - 4v^M}{G^M} p_1 + \frac{S^M}{2G^M} B^\infty \overline{B^\infty} - \frac{m_{\parallel}^M - m_{\perp}^M}{2} (B^\infty)^2 \right] x_2 - \left[\frac{4 - 4v^M}{G^M} a a_1 + \frac{1}{G^M} a b_1 + (m_{\parallel}^M - m_{\perp}^M) B^\infty \overline{\Pi} a^2 \right] \frac{1}{x_2} \\
 & + \left[\frac{1}{G^M} a^3 b_3 - \frac{S^M}{2G^M} \overline{\Pi} \Pi a^4 + \frac{(m_{\parallel}^M - m_{\perp}^M)}{6} \overline{\Pi}^2 a^4 \right] \frac{1}{x_2^3}, \tag{29b}
 \end{aligned}$$

$$u_2^I = \left[\frac{3 - 4v^I}{G^I} \frac{c_1}{a} - \frac{1}{G^I} \frac{\overline{c_1}}{a} + \frac{1}{G^I} \frac{d_1}{a} + \frac{S^I}{2G^I} \Gamma \overline{\Gamma} - \frac{m_{\parallel}^I - m_{\perp}^I}{2} (\overline{\Gamma})^2 \right] x_2 - \left[\frac{3 - 4v^I}{G^I} \frac{c_3}{a^3} - 3 \frac{1}{G^I} \frac{\overline{c_3}}{a^3} \right] x_2^3. \tag{29c}$$

It can also be verified that this solution reduces to that of the perfect interfacial conditions (Wan et al., 2004), if the interfacial stiffness k_n and k_τ tend to be infinite. To find the effective magnetostriction of the composite, which is usually a material constant and independent of external loadings, a strong enough magnetic field is

supposed to be exerted at infinity so that the matrix and inclusion deform with the saturation magnetostriction, i.e.

$$\lambda_{\parallel}^{\text{MS}} = m_{\parallel}^{\text{M}} B^{\infty} \overline{B^{\infty}}, \quad (30a)$$

$$\lambda_{\perp}^{\text{MS}} = m_{\perp}^{\text{M}} B^{\infty} \overline{B^{\infty}}, \quad (30b)$$

$$\lambda_{\parallel}^{\text{IS}} = m_{\parallel}^{\text{I}} B^{\infty} \overline{B^{\infty}}, \quad (31a)$$

$$\lambda_{\perp}^{\text{IS}} = m_{\perp}^{\text{I}} B^{\infty} \overline{B^{\infty}}, \quad (31b)$$

where $\lambda_{\parallel}^{\text{MS}}$ and $\lambda_{\perp}^{\text{MS}}$ are the saturation magnetostriction along the direction of magnetic field and its perpendicular direction for the matrix material, while $\lambda_{\parallel}^{\text{IS}}$ and $\lambda_{\perp}^{\text{IS}}$ are the corresponding saturation magnetostriction for the inclusion. Similar to the previous definition (Herbst et al., 1997; Wan et al., 2004), the effective magnetostriction of the composite can be defined as

$$\lambda^* = \frac{\lambda_{\text{c}}}{\lambda_0}, \quad (32a)$$

where

$$\lambda_{\text{c}} = \frac{1}{\lambda_{\parallel}^{\text{IS}}} \frac{u_2^{\text{M}}|_{x_1=0}}{x_2}, \quad (32b)$$

$$\lambda_0 = \frac{1}{\lambda_{\parallel}^{\text{IS}}} \frac{u_2^{\text{I}}|_{x_1=0}}{a}, \quad (32c)$$

and

$$\begin{aligned} \frac{u_2^{\text{M}}|_{x_1=0}}{x_2} = & \left[\frac{2-4\nu^{\text{M}}}{G^{\text{M}}} p_1 + \frac{S^{\text{M}}}{2G^{\text{M}}} B^{\infty} \overline{B^{\infty}} - \frac{m_{\parallel}^{\text{M}} - m_{\perp}^{\text{M}}}{2} (B^{\infty})^2 \right] - \left[\frac{4-4\nu^{\text{M}}}{G^{\text{M}}} \frac{1}{a} a_1 + \frac{1}{G^{\text{M}}} \frac{1}{a} b_1 + (m_{\parallel}^{\text{M}} - m_{\perp}^{\text{M}}) B^{\infty} \overline{\Pi} \right] f \\ & + \left[\frac{1}{G^{\text{M}}} \frac{1}{a} b_3 - \frac{S^{\text{M}}}{2G^{\text{M}}} \overline{\Pi} \Pi + \frac{(m_{\parallel}^{\text{M}} - m_{\perp}^{\text{M}})}{6} \overline{\Pi}^2 \right] f^2, \end{aligned} \quad (33)$$

where $f = \left(\frac{a}{x_2}\right)^2$, which can be regarded as the volume fraction of inclusion, for the plane case.

4. Results and discussion

In the following discussions, without loss of generality, the Poisson's ratio ν of the materials, including the inclusion, binder and the matrix, and the magnetic Poisson's ratio q of both the inclusion and matrix are all assumed to be 0.3, i.e. $\nu^{\text{I}} = \nu^{\text{M}} = \nu^{\text{b}} = 0.3$, $q^{\text{I}} = q^{\text{M}} = 0.3$. The effective magnetostriction, λ^* , is plotted against the volume fraction, f , for different interfacial stiffness (see Fig. 4). For the sake of comparison, the perfect interface case (Wan et al., 2004) is also plotted. It can be found that as the interfacial stiffness increases, the perfect interface case is more closely approached. The perfect interface is the limit case that can be recovered by choosing the stiffness to be infinite. Fig. 5 is the plot of the effective magnetostriction against the interfacial stiffness. This graph shows that, for a certain volume fraction, a stiffer interfacial layer will always lead to a larger effective magnetostriction, despite that there is a gradual saturation trend of the effective magnetostriction when the stiffness of the interfacial layer becomes very large. Therefore, the interfacial stiffness has obvious influences on the effective magnetostriction of composite, especially when the stiffness is not very high compared with the modulus of matrix. In the case illustrated in Fig. 5, it seems that the influence becomes very obvious when the relative stiffness, $k_{\text{n}}a/E^{\text{M}}$, lies below 3, while this range may vary with different kinds of materials and binder layers.

To design the binder layer, it is important to consider two factors, i.e. the modulus and the thickness of the binder layer, both of which, in terms of Eqs. (5) and (7), obviously influence the equivalent interface stiffness.

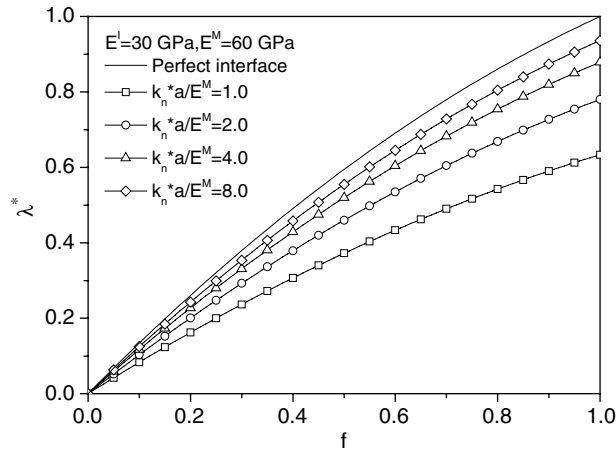


Fig. 4. General relation of the effective magnetostriction and the volume fraction.

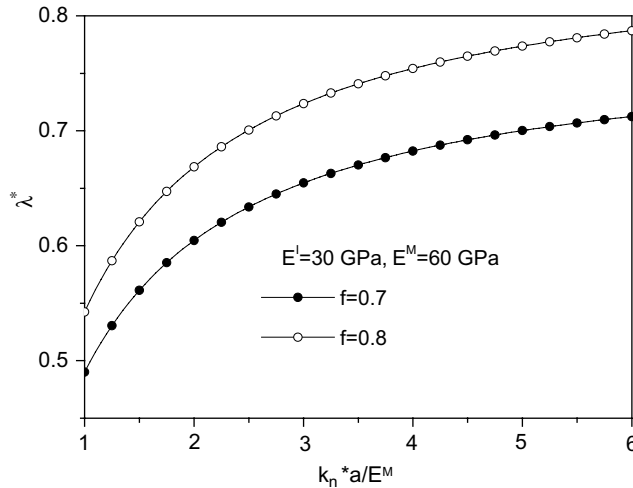


Fig. 5. Interface stiffness, k_n , dependence of the effective magnetostriction, λ^* .

In order to quantitatively understand the influence of the binder layer on the effective magnetostriction of composite, a typical kind of composite is chosen with Terfenol-D as the magnetostrictive phase, glass as the matrix. The moduli of materials are: $E^I = 30$ GPa, $E^M = 50$ GPa. To improve the interfacial stiffness and therefore enhance the effective magnetostriction, one way is to increase the modulus of the binder material. As is shown in Fig. 6, where the effective magnetostriction λ^* is plotted against the binder modulus normalized by the matrix modulus, E^b/E^M , for three different volume fractions $f = 0.3$, $f = 0.5$ and $f = 0.7$, while the binder thickness is fixed to be $\Delta/a = 0.1$, it can be seen that the effective magnetostriction depends monotonously on the binder modulus. A binder with a larger modulus will produce a bigger effective magnetostriction. The effective magnetostriction is obviously influenced by the binder modulus when the modulus is relatively small compared to the matrix. For an example, in the case shown in Fig. 6, the effective magnetostriction obviously decreases as the modulus of binder reduces when the modulus is less than 0.3 times that of the matrix. As is known, in order to obtain a well-fitting property, a flexible binder is usually adopted in the design of magnetostrictive composite. This analysis indicates that the binder layer should be adequately designed so that not too much of the effective magnetostriction is lost while keeping a well-fitting property.

For a certain kind of binder material, another way to improve the interfacial stiffness is to reduce the layer thickness. Choosing epoxy resin as the binder, $E^b = 2$ GPa, and the same materials for the inclusion and

matrix in Fig. 6, Fig. 7 shows the effective magnetostriction (λ^*) plotted against the binder thickness (Δ). It can be seen that the effective magnetostriction generally decreases as the binder layer becomes thicker. For a certain volume fraction, the perfect interface case, which is characterized by zero thickness of the binder, has the maximum effective magnetostriction. The gap is quite large between the effective magnetostriction when the binder layer thickness is 10% of the radius of inclusion and that of the perfect interface case.

To predict the macroscale magnetostriction of Terfenol-D composites, comparison is made between the theoretical predictions and the experimental results in Chen et al. (1999) (see for Fig. 8), where the saturation magnetostriction of Terfenol-D is $\lambda_{\parallel}^{IS} = 930 \times 10^{-6}$ and the matrix has no magnetostriction, $\lambda_{\parallel}^{MS} = 0$. The Young's modulus of the magnetostrictive phase and the matrix are $E^I = 30$ GPa and $E^M = 50$ GPa, respectively. For the sake of comparison, the perfect interface model in Wan et al. (2004) is also presented. Two different kinds of interfacial layer were presented since the interfacial conditions are not clearly known for the experiment. It can be seen that the experimental results are close to the theoretical predictions if the weak interface of a certain stiffness is considered in the model for this kind of magnetostrictive composite, which means that to some extent the model can qualitatively predict the experimental results.

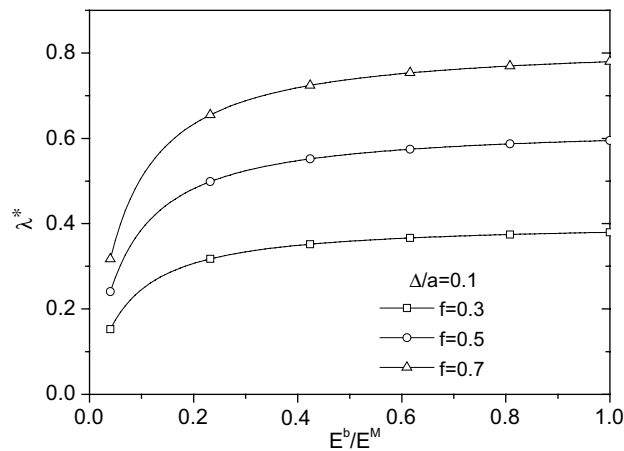


Fig. 6. The binder modulus (E^b) dependence of the effective magnetostriction (λ^*).

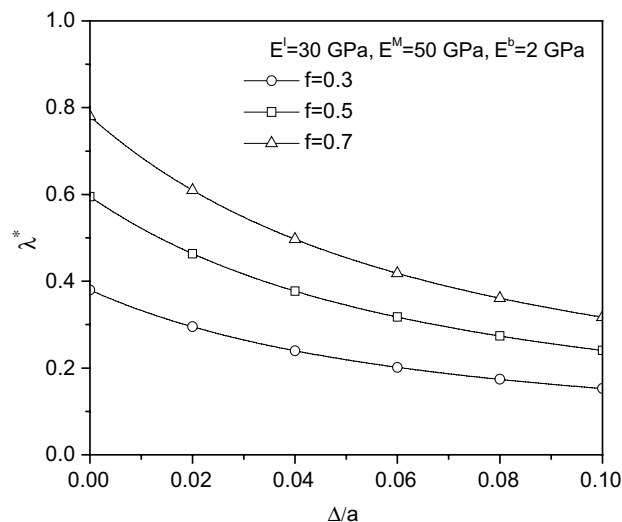


Fig. 7. Binder layer thickness (Δ/a) dependence of the effective magnetostriction (λ^*).

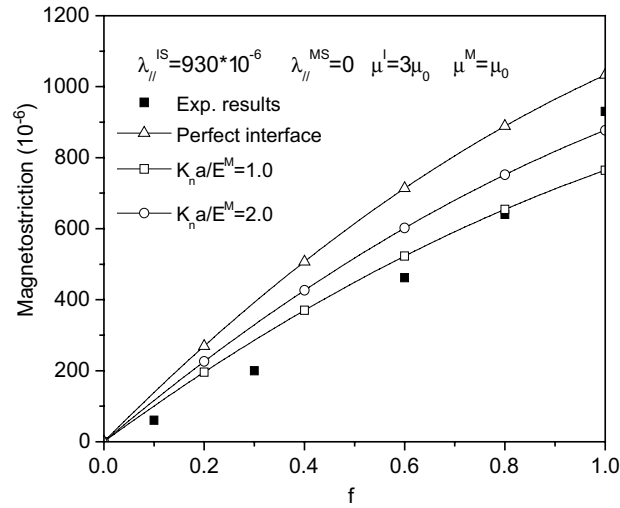


Fig. 8. Comparison with the experimental results in Chen et al. (1999).

5. Conclusions

Magnetostrictive composites with RE metallic alloy particles as magnetostrictive phase have received much attention in recent years. The resin binders are usually used in the preparation of RE magnetostrictive composite. The binders, which are mechanically weak, generally have significant influences on the overall effective magnetostriction of composite. In this paper, this mechanically weak layer of a certain thickness is theoretically modeled by a set of springs with an equivalent stiffness, and the influences of the binder layer on the effective magnetostriction have been discussed. Results show that the interfacial stiffness has significant influences on the effective magnetostriction of the composite. Increasing the interfacial stiffness will obtain a higher effective magnetostriction. Two factors are responsible for the interfacial stiffness, the modulus and the thickness of the binder. A higher modulus or a smaller thickness will lead to a larger interfacial stiffness, and hence, a higher effective magnetostriction.

Acknowledgements

The authors gratefully acknowledge the anonymous reviewers, whose suggestions led to significant improvements of this paper. This work was supported by National Natural Science Foundation of China (Project nos. 10402028, 10432030) and Specialized Research Fund for the Doctoral Program of Higher Education (Project no. 20050247003).

Appendix A

The mathematical formulation of magnetoelasticity with the standard square constitutive relation of magnetostriction can be brought into complex variable framework (Wan et al., 2003b, 2004). The stresses, displacements and resultant force can be expressed with the complex potentials as follows:

$$\sigma_{11} + \sigma_{22} = 4 \left[\Omega'(z) + \overline{\Omega'(z)} - \frac{S}{2} w'(z) \overline{w'(z)} \right], \quad (\text{A.1})$$

$$\sigma_{22} - \sigma_{11} + 2\sigma_{12}i = 4 \left[\bar{z}\Omega''(z) + \Psi'(z) - \frac{S}{2} w''(z) \overline{w'(z)} \right], \quad (\text{A.2})$$

$$T_1 + iT_2 = -2i \left[\Omega(z) + z\overline{\Omega'(z)} + \overline{\Psi(z)} - \frac{S}{2} w(z) \overline{w'(z)} \right]_{z_0}, \quad (\text{A.3})$$

$$u_1 + iu_2 = \frac{3-4\nu}{G} \Omega(z) - \frac{1}{G} z\overline{\Omega'(z)} - \frac{1}{G} \overline{\Psi(z)} + \frac{S}{2G} w(z) \overline{w'(z)} + \frac{m_{\parallel} - m_{\perp}}{2} \int \overline{[w'(z)]^2} dz, \quad (\text{A.4})$$

where $\Omega(z)$ and $\Psi(z)$ are complex potentials, which are given in Eqs. (28a) and (28b) for the matrix, Eqs. (28c) and (28d) for the inclusion, respectively, for the problem described in this paper. $w(z)$ is the complex potential of magnetic induction, which is presented in Eq. (1a) for the matrix and Eq. (1b) for the inclusion, respectively. The symbol S is a combination of parameters given in Eq. (22). A prime represents the derivative with respect to the complex variable, z . The resultant force is integration of the surface tractions along the interface, i.e. $T_1 + iT_2 = \int (t_1 + it_2) ds$.

Appendix B

The relation between the coefficients a_0, b_0, c_0, d_0, b_2 and c_2 are as follows:

$$\frac{k_n}{G^M} (3 - 4\nu^M) \bar{a}_0 - \frac{k_n}{G^M} b_0 - \frac{k_n}{G^I} (3 - 4\nu^I) \bar{c}_0 + \frac{k_n}{G^I} d_0 - \frac{k_n}{G^M} \bar{b}_2 - \left[\frac{k_n}{G^I} (1 - 4\nu^I) + \frac{4}{a} \right] c_2 = 0, \quad (\text{B.1})$$

$$- \frac{k_\tau}{G^M} (3 - 4\nu^M) \bar{a}_0 + \frac{k_\tau}{G^M} b_0 + \frac{k_\tau}{G^I} (3 - 4\nu^I) \bar{c}_0 - \frac{k_\tau}{G^I} d_0 - \frac{k_\tau}{G^M} \bar{b}_2 - \left[\frac{k_\tau}{G^I} (5 - 4\nu^I) + \frac{4}{a} \right] c_2 = 0, \quad (\text{B.2})$$

$$- a_0 - \bar{b}_0 + c_0 + \bar{d}_0 + 2\bar{c}_2 = 0, \quad (\text{B.3})$$

$$- \bar{b}_2 + c_2 = 0, \quad (\text{B.4})$$

from which b_2 and c_2 can be solved to be zero, i.e. $b_2 = c_2 = 0$. To eliminate the rigid displacements, one can generally set the displacement of the origin ($z = 0, \zeta = 0$) to be zero, i.e. $(u_1 + iu_2)|_{\zeta=0} = 0$. Therefore, the following equation can be arrived:

$$\frac{3 - 4\nu^I}{G^I} c_0 - \frac{1}{G^I} \bar{d}_0 = 0. \quad (\text{B.5})$$

Together with the supplementary Eq. (B.5), the coefficients of a_0, b_0, c_0, d_0 are linked by

$$\frac{3 - 4\nu^M}{G^M} a_0 - \frac{1}{G^M} \bar{b}_0 = 0, \quad (\text{B.6})$$

$$\frac{3 - 4\nu^I}{G^I} c_0 - \frac{1}{G^I} \bar{d}_0 = 0, \quad (\text{B.7})$$

$$a_0 + \bar{b}_0 = c_0 + \bar{d}_0. \quad (\text{B.8})$$

Without loss of generality, setting one of these coefficients to be zero, e.g. $a_0 = 0$, then all the others three coefficients b_0, c_0, d_0 vanish. The equations of $a_{k-2}, b_k, c_k, d_{k-2}$ ($k \geq 4$) are listed as follows:

$$\left[\frac{k_n}{G^M} (3 - 4\nu^M) + \frac{k_n}{G^M} (k - 2) \right] \bar{a}_{k-2} - \frac{k_n}{G^M} \bar{b}_k + \left[\frac{2}{a} (k - 3)k - \frac{k_n}{G^I} (3 - 4\nu^I) + \frac{k_n}{G^I} k \right] c_k + \left[\frac{2}{a} (k - 2) + \frac{k_n}{G^I} \right] d_{k-2} = 0, \quad (\text{B.9})$$

$$\left[\frac{k_\tau}{G^M} (3 - 4\nu^M) - \frac{k_\tau}{G^M} (k - 2) \right] \bar{a}_{k-2} + \frac{k_\tau}{G^M} \bar{b}_k + \left[\frac{2}{a} (k - 1)k + \frac{k_\tau}{G^I} (3 - 4\nu^I) + \frac{k_\tau}{G^I} k \right] c_k + \left[\frac{2}{a} (k - 2) - \frac{k_\tau}{G^I} \right] d_{k-2} = 0, \quad (\text{B.10})$$

$$(k - 2) \bar{a}_{k-2} - \bar{b}_k + c_k = 0, \quad (\text{B.11})$$

$$- \bar{a}_{k-2} + kc_k + d_{k-2} = 0. \quad (\text{B.12})$$

It can be easily found that all the coefficients $a_{k-2}, b_k, c_k, d_{k-2}$ ($k \geq 4$) equal zero.

References

Chen, Y., Snyder, J.E., Schwichtenberg, C.R., Dennis, K.W., Falzgraf, D.K., McCallum, R.W., Jiles, D.C., 1999. Effect of the elastic modulus of the matrix on magnetostrictive strain in composites. *Applied Physics Letters* 74, 1159–1161.

- Clark, A.E., 1980. Magnetostrictive rare earth-Fe₂ compounds. In: Wohlfarth, E.P. (Ed.), *Ferromagnetic Materials*, vol. 1. North-Holland Publishing Company, Amsterdam.
- Dong, S.X., Zhai, J.Y., Xing, Z.P., Li, J.F., Viehland, D., 2005. Extremely low frequency response of magnetoelectric multilayer composites. *Applied Physics Letters* 86, 102901.
- Duenas, T.A., Carman, G.P., 2001. Particle distribution study for low-volume fraction magnetostrictive composites. *Journal of Applied Physics* 90, 2433–2439.
- Guo, Z.J., Busbridge, S.C., Piercy, A.R., Zhang, Z.D., Zhao, X.G., Wang, B.W., 2001. Effective magnetostriction and magnetomechanical coupling of Terfenol-D composites. *Applied Physics Letters* 78, 3490–3492.
- Herbst, J.F., Capehart, T.W., Pinkerton, F.E., 1997. Estimating the effective magnetostriction of a composite: a simple model. *Applied Physics Letters* 70, 3041–3043.
- Hudson, J., Busbridge, S.C., Piercy, A.R., 1998. Magnetomechanical coupling and elastic moduli of polymer-bonded Terfenol composites. *Journal of Applied Physics* 83, 7255–7257.
- Kendall, D., Piercy, A.F.L., 1993. The frequency dependence of eddy current losses in Terfenol-D. *Journal of Applied Physics* 73, 6174–6176.
- Kim, S.R., Kang, S.Y., Park, J.K., Nam, J.T., Son, D., Lim, S.H., 1998. Magnetostrictive properties of polymer-bonded amorphous Tb–Fe–B composites. *Journal of Applied Physics* 83, 7285–7287.
- Nan, C.W., 1998. Effective magnetostriction of magnetostrictive composites. *Applied Physics Letters* 72, 2897–2899.
- Pao, Y.H., Yeh, C.S., 1973. A linear theory for soft ferromagnetic elastic solids. *International Journal of Engineering Science* 11, 415–436.
- Ren, W.J., Or, S.W., Chan, H.L.W., Zhang, Z.D., 2005. Magnetoelastic properties of polymer-bonded Sm_{0.88}Dy_{0.12}Fe_{1.93} pseudo-1–3 composites. *Journal of Magnetism and Magnetic Materials* 293, 908–912.
- Wan, Y.P., Fang, D.N., Hwang, K-Ch., 2003a. Nonlinear constitutive relations for the magnetostrictive materials. *International Journal of Non-linear Mechanics* 38, 1053–1065.
- Wan, Y.P., Fang, D.N., Soh, A.K., Hwang, K-Ch., 2003b. Effects of magnetostriction on fracture of a soft ferromagnetic medium with a crack-like flaw. *Fatigue and Fracture of Engineering Materials & Structures* 26, 1091–1102.
- Wan, Y.P., Zhong, Z., Fang, D.N., 2004. Permeability dependence of the effective magnetostriction of magnetostrictive composites. *Journal of Applied Physics* 95, 3099–3110.
- Zheng, X.J., Liu, X.E., 2005. A nonlinear constitutive model for Terfenol-D rods. *Journal of Applied Physics* 97, 053901.